HHS Public Access

Author manuscript

Brain Res. Author manuscript; available in PMC 2020 March 15.

Published in final edited form as:

Brain Res. 2019 March 15; 1707: 198–207. doi:10.1016/j.brainres.2018.11.039.

miR-146a Mediates Thymosin β4 Induced Neurovascular Remodeling of Diabetic Peripheral Neuropathy in Type-II Diabetic Mice

Lei Wang[1], **Michael Chopp**[1,3], **XueRong Lu**[1], **Alexandra Szalad**[1], **LongFei Jia**[1], **Xian Shuang Liu**[1], **Kuan-Han Wu**[2], **Mei Lu**[2], and **Zheng Gang Zhang**[1]

[1]Department of Neurology, Henry Ford Hospital, 2799 W. Grand Boulevard, Detroit, Michigan 48202

[2]Department of Biostatistics and Research Epidemiology, Henry Ford Hospital, 2799 W. Grand Boulevard, Detroit, Michigan 48202

[3]Department of Physics, Oakland University, Rochester, Michigan 48309

Abstract

Diabetes induces neurovascular dysfunction leading to peripheral neuropathy. MicroRNAs (miRNAs) affect many biological processes and the development of diabetic peripheral neuropathy. In the present study, we investigated whether thymosin-β4 (Tβ4) ameliorates diabetic peripheral neuropathy and whether miR-146a mediates the effect of Tβ4 on improved neurovascular function. Male Type II diabetic BKS.Cg-*m*+/+*Lepr*^{db}/*J* (db/db) mice at age 20 weeks were treated with Tβ4 for 8 consecutive weeks, and db/db mice treated with saline were used as a control group. Compared to non-diabetic mice, diabetic mice exhibited substantially reduced miR-146a expression, and increased IL-1R-associated kinase-1 (IRAK1), tumor necrosis factor (TNFR)-associated factor 6 (TRAF6) levels and nuclear factor kappa-light-chain-enhancer of activated B cells (NFkB) activity in sciatic nerve tissues. Treatment of diabetic mice with Tβ4 significantly elevated miR-146a levels and overcame the effect of diabetes on these proteins. Tβ4 treatment substantially improved motor and sensory conduction velocity of the sciatic nerve, which was associated with improvements in sensory function. Tβ4 treatment significantly increased intraepidemal nerve fiber density and augmented local blood flow and the density of fluorescein isothiocyanate (FITC)-dextran perfused vessels in the sciatic nerve tissue. In vitro, treatment of dorsal root ganglion (DRG) neurons and mouse dermal endothelial cells (MDEs) with Tβ4 significantly increased axonal outgrowth and capillary-like tube formation, whereas blocking miR-146a attenuated Tβ4-induced axonal outgrowth and capillary tube formation, respectively.

Please send all correspondence to: Dr. Lei Wang, Department of Neurology, Henry Ford Hospital, 2799 West Grand Boulevard, Detroit, MI 48202, Tel: 313-916-9443, Fax:313-916-1318, leiwang@neuro.hfh.edu.

Author Contributions statement

All authors have read and approved submission of our manuscript. Conceived and designed the experiments: LW, MC, ZGZ. Performed the experiments: LW, XL, AS, LJ, XSL. Analyzed the data: LW AS KW ML. Wrote the paper: LW, MC, ZGZ.

Declaration of Conflicting Interests: none

Our data indicate that miR-146a may mediate Tβ4-induced neurovascular remodeling in diabetic mice, by suppressing pro-inflammatory signals.

Keywords

Thymosin β4; miR-146a; diabetes; peripheral neuropathy; mice

1. Introduction

Diabetic peripheral neuropathy is a significant complication of diabetes. The vast majority of people with diabetes have type II diabetes. Type II diabetes is associated with subclinical inflammation and activation of the innate immune system (Pickup, 2004). Diabetic patients with peripheral neuropathy have increased serum levels of inflammatory cytokines (Bilir et al., 2016; Doupis et al., 2009). Hyperglycemia activates pro-inflammatory mediators, which induce vascular dysfunction and nerve damage. Inflammatory mediators participate in the pathogenesis of diabetic peripheral neuropathy (Kawamura et al., 2008; Wright, 2011).

Thymosin β4 (Tβ4), a small acidic polypeptide, has multiple biological functions including neurorestoration and anti-inflammation (Chopp and Zhang, 2015). Tβ4 promotes central nervous system plasticity and neurovascular remodeling leading to neurological recovery in a variety of neurological diseases (Morris et al., 2010; Xiong et al., 2011). Tβ4 attenuates inflammatory cell infiltration and promotes wound healing in diabetic animals (Evans et al., 2013). Our previous studies have found that Tβ4 ameliorates diabetes-induced neurovascular dysfunction, and thereby promotes neurological recovery of diabetic peripheral neuropathy (Wang et al., 2012; Wang et al., 2015a). However, the mechanisms by which Tβ4 improves neurological outcome in diabetic neuropathy have not been fully investigated.

MicroRNAs (miRNAs) are small non-coding RNAs that are key players in mediating physiological and pathogenesis functions of diabetes mellitus and diabetic complications (Kantharidis et al., 2011; Lorenzen et al., 2012). Dysregulation of miRNAs may affect inflammation and lead to development of diabetic neuropathy (Andersen et al., 2014; Gong et al., 2015). miRNAs are potential biomarkers and therapeutic targets in clinical pain disorders (Andersen et al., 2014). miR-146a modulates inflammatory and innate immunity responses by negatively regulating its target genes IRAK1, TRAF6 and NFkB activation, which subsequently down-regulate pro-inflammatory mediators such as MCP-1 and VCAM-1 (Landry et al., 1997; Taganov et al., 2006). The serum level of miR-146a is significantly decreased in type II diabetic patients (Balasubramanyam et al., 2011; Baldeon et al., 2014). miR-146a attenuates neuropathic pain by suppressing TRAF6 signaling in the spinal cord (Lu et al., 2015). Moreover, miR-146a over-expression represses the endothelial inflammatory response (Cheng et al., 2013). We recently demonstrated that treatment of diabetic db/db mice with miR-146a mimics reduces diabetic peripheral neuropathy (Liu et al., 2017). In addition, the miR-146a increases DRG neuronal survival and axonal outgrowth under hyperglycemia conditions (Jia et al., 2016; Wang et al., 2014). miR-146a upregulated by Tβ4 promotes oligodendrocyte differentiation by suppression of pro-inflammatory pathways (Santra et al., 2014). Furthermore, Tβ4 inhibits the expression and secretion of

inflammatory mediators through miR-146a in hypoxia injured rats (Zhou et al., 2015). However, whether miR-146a mediates the therapeutic effect of Tβ4 on diabetic peripheral neuropathy has not been investigated.

In the present study, we elucidate the molecular mechanisms underlying the therapeutic effect of Tβ4 on diabetic peripheral neuropathy with a focus on miR-146a. We hypothesize that miR-146a is involved in Tβ4-improved neurovascular function in diabetic db/db mice.

2. Results

2.1. Tβ4 reverses the effect of diabetes on miR-146a expression and its target proteins in sciatic nerve tissues.

Our previous study showed that diabetes reduced miR-146a expression in DRG neurons (Wang et al., 2014). To extend our findings, we measured miR-146a levels in sciatic nerve tissues by means of quantitative real time RT-PCR and found that diabetic db/db mice exhibited significantly decreased miR-146a expression compared to that in non-diabetic mice, which was reversed by Tβ4 treatment (Fig. 1). These data indicate that Tβ4 treatment overcomes diabetes-reduced miR-146a expression in the sciatic nerve tissues. IRAK1 and TRAF6 are genes that are targeted by miR-146a (Balasubramanyam et al., 2011; Yousefzadeh et al., 2015). Increasing activity of NFkB regulates the expression of MCP-1 and VCAM-1 (Landry et al., 1997). Thus, we examined the effect of Tβ4 on the expression of these proteins in sciatic nerve tissues. Western blot analysis showed that diabetic db/db mice exhibited a considerable increase in IRAK1 and TRAF6 protein levels, whereas treatment with Tβ4 markedly suppressed these two proteins (Fig. 1). Moreover, Tβ4 substantially reduced phosphorylated NFkB (p-NFkB), MCP-1 and VCAM-1 protein levels in sciatic nerve tissues compared to the saline treatment (Fig. 1). Double immunofluorescent staining revealed that IRAK1 and TRAF6 immunoreactivity was co-localized to vWF positive endothelial cells (Fig. 1). Collectively, these data suggest that Tβ4 reverses the effect of diabetes on miR-146a expression and its target proteins in sciatic nerve tissues.

2.2. Tβ4 ameliorates vascular dysfunction in the sciatic nerve tissues. miR-146a mediates the effect of Tβ4 on endothelial cell tube formation in vitro.

To examine whether Tβ4-regulation of miR-146a and its target proteins promotes vascular remodeling, vascular function was measured. Consistent with a previous report (li et al., 2005; Wang et al., 2012), diabetic db/db mice exhibited substantial reduction of local blood flow in the sciatic nerve tissues, measured by means of a Laser Doppler Flowmeter (LDF) and FITC-dextran perfused functional microvascular density, compared to non-diabetic mice. Treatment of db/db mice with Tβ4 significantly increased functional microvascular density and regional blood flow in the sciatic nerve tissues compared to saline treated db/db mice (Fig.2). To further examine whether miR-146a mediates Tβ4-improved vascular function, we performed an in vitro capillary tube formation assay in MDEs. Compared to normal glucose (5 mM), high glucose conditions (30 mM) significantly reduced capillary tube formation. Application of Tβ4 to MDEs overcame the inhibitory effect on capillary tube formation induced by high glucose, whereas attenuation of endogenous miR-146a by siRNA against miR-146a abolished the effect of Tβ4 on endothelial cell capillary tube

formation compared to the scramble negative control (Fig.2). Quantitative real-time RT-PCR and Western blot analysis showed that the transfection of MDEs with miR-146a mimics markedly increased the miR-146a level, and reduced the protein levels of IRAK1 and TRAF6 compared to the miR-146a mimic control, respectively (Fig.2). MDEs cultured under a high glucose condition exhibited substantially reduced miR-146a and increased miR-146a target mRNAs and proteins, IRAK1 and TRAF6 and p-NFkB, along with increased MCP-1 and VCAM-1 expression, respectively. However, addition of Tβ4 reversed the effect of high glucose on miR-146a and its target mRNAs and proteins in MDEs. Furthermore, blockage of endogenous miR-146a attenuated Tβ4-suppressed IRAK1, TRAF6 and p-NFkB, as well as MCP-1 and VCAM-1 expression (Fig.2). These in vitro data suggest that miR-146a contributes to Tβ4 improved vascular function likely via its target proteins IRAK1 and TRAF6, and downstream NFkB signaling.

2.3. miR-146a mediates the effect of Tβ4 on axonal outgrowth in DRG neurons.

To test whether miR-146a is involved in Tβ4-induced axonal remodeling in diabetic mice, we measured intraepidermal nerve fiber density on plantar skin tissues. Diabetic mice exhibited reduction of PGP9.5 positive intraepidermal sensory nerve fibers, and Tβ4 significantly augmented intraepidermal nerve fiber density in diabetic mice compared to saline treatment (Fig.3), which is consistent with a prior report (Wang et al., 2015a).

We performed in vitro experiments to examine the effect of miR-146a on Tβ4 induced DRG neuron axonal growth, using a microfluidic device which separates distal axons from their parent neuronal soma (Jia et al., 2016; Zhang et al., 2013). DRG neurons cultured under a high glucose condition exhibited substantial suppression of axonal outgrowth, which was overcome by application of Tβ4. However, attenuation of endogenous miR-146a in DRG neurons with siRNA against miR-146a significantly reduced Tβ4-enhanced DRG axonal growth compared to the scramble negative control group (Fig.3). Quantitative real-time RT-PCR revealed that high glucose reduced DRG neuron miR-146a levels and substantially increased miR-146a target genes, IRAK1 and TRAF6 in DRG neurons. However, Tβ4 significantly reversed high glucose-reduced miR-146a levels and the high glucose-increased IRAK1 and TRAF6 expression. siRNA against miR-146a in DRG neurons attenuated Tβ4-decreased IRAK1 and TRAF6 mRNA levels (Fig.3). The data indicate that miR-146a mediates Tβ4-induced axonal outgrowth under hyperglycemia.

2.4. Tβ4 improves neurological function in diabetic db/db mice.

Next, we investigated whether augmentation of neurovascular remodeling by Tβ4 affects neurological function of diabetic neuropathy. Consistent with our previous report (Wang et al., 2012), Tβ4-treatment significantly improved motor and sensory conduction velocities (MCV and SCV) in the sciatic nerve, and thermal latency (Plantar test) compared to diabetic db/db mice treated with saline (Fig.4). However, Tβ4-treatment in db/db mice did not decrease blood glucose and body weight (Table 1 and 2).

3. Discussion

The present study observed that miR-146a expression was considerably reduced in sciatic nerve tissues of diabetic db/db mice, and this reduction was associated with an increase in its target proteins IRAK1 and TRAF6, and NFkB activation, resulting in increased MCP-1 and VCAM-1 levels. Treatment of diabetic peripheral neuropathy with Tβ4 significantly upregulated miR-146a levels and suppressed expression of miR-146a target pro-inflammatory mediators, as well as improved neurovascular remodeling in diabetic db/db mice. In vitro, inhibiting endogenous miR-146a attenuated the effect of Tβ4-induced capillary tube formation and axonal outgrowth in MDEs and DRG neurons under high glucose conditions, respectively. These data provide a molecular mechanism, that miR-146a via its target genes, likely mediates the therapeutic effect of Tβ4 on diabetic neuropathy.

Diabetic patients and rodents experience an increase in inflammatory mediators including cytokines, chemokines and adhesion molecules that are primarily produced by activated immune cells, macrophages and adipocytes (King, 2008; Navarro and Mora, 2005; Newton and Dixit, 2012). Inflammatory mediators create a pro-inflammatory microenvironment that leads to neurovascular dysfunction in the peripheral nerve system (Rahman et al., 2016). Diabetic neuropathy exhibits features of chronic subclinical inflammation. There is a significant correlation between increases in pro-inflammatory signals of NFkB, MCP-1 and VCAM-1 and diabetic peripheral neuropathy (Guan et al., 2011; Hocaoglu-Emre et al., 2017; Wright, 2011). Inhibition of the inflammatory mediators is effective in improving peripheral nerve and vascular function in diabetic neuropathy (Zhou and Zhou, 2014), and thereby constitutes a possible therapeutic target for diabetic neuropathy.

Dysregulation of miRNAs has been reported in human and animal models of diabetic neuropathy (Andersen et al., 2014; Gong et al., 2015). miRNAs may contribute to the pathogenesis of diabetic neuropathy (Gong et al., 2015; Natarajan et al., 2012). miR-146a regulates immune and inflammation response (Bhaumik et al., 2008; Hou et al., 2009). Serum levels of miR-146a are reduced in type II diabetic patients (Baldeon et al., 2014). miR-146a has been found to be a susceptibility factor in diabetic neuropathy (Ciccacci et al., 2014). miR-146a and its target genes IRAK1 and TRAF6 are involved in the pathogenesis of diabetic neuropathy (Yousefzadeh et al., 2015). Our previous study demonstrated that systemic administration of exogenous miR-146a mimics to diabetic db/db mice with peripheral neuropathy robustly improved regional blood flow in sciatic nerve tissue and neurological outcome by suppressing expression of IRAK1, TRAF6 and inactivating downstream NFkB signaling in the sciatic nerve tissue (Liu et al., 2017). Moreover, our previous in vitro studies have demonstrated that miR-146a mediates Tβ4-increased oligodendrogenesis via inhibiting IRAK1/TRAF6 and modulating the p38 MAPK pathway (Santra et al., 2014), while an increased miR-146a promotes axonal growth of DRG neurons under high glucose condition by targeting IRAK1 and TRAF6 (Jia et al., 2016). The current study confirms and extends the published studies by showing that miR-146a elevated by Tβ4 mediates the therapeutic effect of improvement of neurovascular function in diabetic neuropathy via suppressing pro-inflammatory signaling of IRAK1, TRAF6, and NFkB. The specificity for miR-146a to target IRAK1 and TRAF6 has been demonstrated (Hou et al., 2009; Liu et al., 2017; Taganov et al., 2006). There are two nucleotide differences of seed

regions between miR-146a and miR-146b, although they are located in different chromosomes (Garcia et al., 2011). Both miR-146a and miR-146b share the same effects on their targeted genes including BRCA1 in breast cancer cells (Garcia et al., 2011). Thus, it is likely that TRAF6 and IRAK1 genes targeted by miR-146a mimics can be targeted by miR-146b. We do not exclude the possibility that other miRNAs may also be involved in the beneficial effects of Tβ4 in diabetic neuropathy. Therefore, additional studies are warranted.

Diabetic neuropathy is closely associated with marked neurovascular dysfunction (Davidson et al., 2018; Yorek, 2015). Neurorestorative effects in diabetic peripheral neuropathy are mediated by many coupled events, including vascular remodeling and axonal outgrowth; each factor impacts the others. Our in vitro data indicate that miR-146a and its target proteins mediate the augmentation of vascular function and axonal outgrowth by Tβ4. In vivo, the present study shows that Tβ4-improved microvascular and axonal remodeling is tightly coupled, and both, in concert, likely contribute to improved neurological outcome. However, additional studies are warranted to investigate the cause-effect and sequence of vascular and axonal remodeling induced by Tβ4. Based on the present data and published studies, we speculate that Tβ4-upregulated miR-146a represses IRAK1 and TRAF6, resulting in attenuation of NF-kB signaling activation including pro-inflammatory mediators, MCP-1 and VCAM-1, consequently ameliorating neurovascular dysfunction and peripheral neuropathy (Fig.5). There are multiple pathways that mediate Tβ4-improved neurovascular function. We previously demonstrated that Tβ4 impacts Ang1/Tie2 and PI3K/AKT signaling pathways (Wang et al., 2012). Here, we found that miR-146a and its target pro-inflammatory factors mediate the Tβ4 therapeutic effect on neurovascular remodeling. Additional studies of diabetic neuropathy are warranted to investigate the effect of Tβ4-increased miR-146a on other signaling pathways such as p38 MAPK.

Diabetic db/db mice develop diabetes at age of 4 weeks, while peripheral neuropathy characterized by slowed NCVs occurs between 8-14 weeks of age (li et al., 2005; Pande et al., 2011; Sima and Robertson, 1978). Morphometric changes including myelinated and unmyelinated fibers and sensory neurons occur after 20 weeks of diabetes, which resembles human diabetic peripheral neuropathy (Norido et al., 1984). Thus, in the present study, 20 week-old diabetic mice were used.

DRG sensory neuron growth has high metabolic requirements (Russell et al., 1999; Russell et al., 2002). We define a normal glucose medium as a medium containing 25 mM, which is the optimal concentration for primary embryonic DRG neuron growth (Jia et al., 2016; Russell et al., 1999; Russell et al., 2002; Wang et al., 2014). However, in vivo, a normal glucose level is approximately 5 mM. Therefore, additional experiments with adult DRG neurons derived from diabetic mice are warranted to mimic in vivo conditions. In contrast to our results, miR-146a expression was increased in the sciatic nerve of STZ induced diabetic rats (Yousefzadeh et al., 2015). The differences in miR-146a expression may be due to differences in animal-type and diabetic model.

In conclusion, we have demonstrated that the treatment of diabetic peripheral neuropathy with Tβ4 significantly promotes neurovascular remodeling, leading to improvement of

neurological function recovery. miR-146a may mediate the therapeutic effects of Tβ4 by suppressing pro-inflammatory mediators.

4. Experimental Procedure

4.1. Animals:

All experimental procedures were approved by the Henry Ford Hospital Institutional Animal Care and Use Committee (IACUC#1486). Adult male BKS. Cg-*m*+/+*Lepr*^{db}/*J* (db/db) mice were used as a model of type II diabetes, and heterozygote mice (db/m, a non-penetrant genotype) served as nondiabetic controls. Mice were purchased from Jackson Laboratories.

4.2. Tβ4 treatment:

Diabetic db/db mice (age 20 weeks) were randomized to intraperitoneal (i.p.) injection with Tβ4 (30 mg/kg, RegeneRx, Inc. n=10/group) daily for 8 weeks. Age-matched db/db mice (n=10/group) and nondiabetic db/m mice (n=10/group) administered with the same volume of saline were employed as control. All mice were sacrificed eight weeks after the initial treatment. The doses and drug delivery route of Tβ4 were determined in previous studies (Wang et al., 2015a; Xiong et al., 2012).

Blood glucose, body weight and functional tests were measured in all mice before the initiation of treatment, and then every 4 weeks. Blood glucose level was assessed using test strips for glucose (Roche Diagnostics). The treatment assignments were blinded to investigators who participated in behavioral tests and endpoint analyses.

4.3. Measurement of motor and sensory nerve conduction velocity:

Nerve conduction velocity of the sciatic nerve was measured with orthodromic recording techniques according to published protocols (li et al., 2005; Wang et al., 2012; Wang et al., 2015b). Briefly, animals were anesthetized with ketamine/xylazine (i.p., 100/10 mg/kg) and their rectal temperature was maintained at 37 ± 1.0°C using a feedback controlled water bath during the measurements. The sciatic notch and knee were stimulated with electrodes via a stimulator (A-M Systems, Model 2100). The simultaneous electromyographies were recorded from the dorsum of the foot by two sterilized electrodes with an Amplifier (Grass Instruments, Model P5). Motor nerve conduction velocity (MCV) and sensory nerve conduction velocity (SCV) were calculated based on published studies (li et al., 2005; Wang et al., 2012; Wang et al., 2015b).

4.4. Measurement of thermal sensitivity:

Plantar test (Hargreaves Method) was performed using the Plantar Test and Tail Flick Analgesia Meter (IITC Life Science, Model 336 TG), as previously described (Wang et al., 2015a; Wang et al., 2015b). Briefly, animals were acclimated for 20 min in a plexiglass chamber resting on a transparent glass surface. The temperature of the floor was set at ~32-33°C (manufacturer's setup). The radiant heat source (15% intensity which produced a heating rate of ~1.3°C per sec) was placed under the hind paw. The paw-withdrawal latency in response to the radiant heat was recorded, with a cut-off time of 30 sec. For each mouse,

five readings were taken at 15 min intervals, and the mean value was calculated (Wang et al., 2015a; Wang et al., 2015b).

4.5. Measurement of regional blood flow and microvascular plasma perfusion:

Regional blood flow in sciatic nerve tissues was assessed by laser Doppler flowmetry (LDF PeriFlux PF4, Perimed AB) after 8 weeks of initial treatment (Wang et al., 2012; Wang et al., 2015b). Briefly, the mouse was mounted on a Kopf stereotaxic apparatus under anesthesia (ketamine/xylazine, i.p., 100/10 mg/kg, JHP Pharmaceuticals LLC.). The left sciatic nerve tissue in the mid-thigh region was exposed and the temperature of these mice was maintained at 37 ± 1.0°C by a water bath. Relative flow values expressed as perfusion units were measured using the LDF probe placed at the surface of the sciatic nerve, every 5 minutes for a total of 5 recordings. Regional blood flow values in sciatic nerve tissues from non-diabetic db/m mice are defined as baseline values and data are expressed as a percentage of baseline values (Wang et al., 2012; Wang et al., 2015b). To assess blood perfusion in the sciatic nerve, fluorescein isothiocyanate (FITC)-dextran (0.2 mL of 50 mg/mL, 2×10^6 molecular weight, Sigma Aldrich) was intravenously (i.v.) injected to the mice (Wang et al., 2012; Wang et al., 2015b). Ten minutes later, the sciatic nerve tissues were rapidly harvested and fixed in 2% of paraformaldehyde for 2 hours. The whole mount sciatic nerves were digitized under a 10x objective using a laser-scanning confocal microscope (Zeiss LSM 510 NLO, Carl Zeiss) (Wang et al., 2012; Wang et al., 2015b). The sciatic nerves were then embedded in optimum cutting temperature (OCT) compound and 20 μm thickness cross sections were cut. They were imaged under a 20x microscope objective (Zeiss Axiophot) via a Micro Computer Imaging Device (MCID) system (Imaging Research Inc.). Three sections at 60 μm intervals from each nerve were applied. The vascular density was expressed as the total number of FITC-dextran perfused vessels divided by the total tissue-area (mm^2) (Wang et al., 2012; Wang et al., 2015b).

4.6. Immunohistochemistry:

For immunohistochemistry, the sciatic nerves were fixed in 4% paraformaldehyde and then embedded in paraffin (Wang et al., 2012). Footpad skin was fixed in ice-cold Zamboni's fixative for 2 hours and then kept in 30% sucrose/PBS overnight at 4°C. The skin samples were then frozen in OCT compound. Three longitudinal 6-μm-thick sciatic nerve and 20-μm-thick footpad sections from each animal were used (Wang et al., 2015b). For immunostaining, the following primary antibodies were applied: polyclonal rabbit anti-protein gene product 9.5 (PGP9.5, 1:1,000, MILLIPORE), polyclonal rabbit anti-Von Willebrand Factor (vWF, 1:300, Dako), polyclonal rabbit anti-IRAK1 (1:50, Santa Cruz Biotech) and polyclonal rabbit anti-TRAF6 (1: 50, Santa Cruz Biotech). Rabbit anti-IgG was applied as a negative control. 4′ 6-Diamidino-2-phenylindole (DAPI, 1:5000, Thermo Scientific) was used as a nuclear counterstain.

4.7. Image acquisition and quantification:

To measure intraepidermal nerve fiber density (IENFD), nerve profiles were imaged under a 40x microscope objective (Carl Zeiss Axiostar Plus Microscope) using the MCID system. The number of nerve fibers crossing the dermal-epidermal junction were measured and

interepidermal nerve fiber density was presented as number of fibers per millimeter of length of epidermis (Wang et al., 2015b).

4.8. Capillary-like tube formation assay:

The capillary-like tube formation assay was performed to examine the effect of Tβ4 on in vitro angiogenesis (Wang et al., 2012). Briefly, Mouse Dermal Microvascular Endothelial Cells (MDEs, Cell Biologics Inc.) were cultured in regular (5 mM) or high (30 mM) glucose conditions with or without 100 ng/ml of Tβ4 for 48 hours. MDEs (2×10^4 cells) were seeded on Matrigel-coated-96-well plate (BD Biosciences) for 5 hours. Total length of tubes in 3 randomly selected fields/well was assessed using the MCID system (Wang et al., 2012). Experiments were repeated 6 times, independently (n=6/group). In the MDE study, a regular glucose (RG) medium was referred to as a medium containing 5 mM glucose, while a high glucose (HG) medium was defined as a medium containing 30 mM glucose, which was chosen to match glucose levels prevalent in patients with uncontrolled diabetes (Wang et al., 2012; Wu et al., 1999).

4.9. Culture of primary embryonic DRG neurons:

Primarily DRG neurons were harvested from embryonic day 18 Wistar rats (ED18, either sex; Charles River Laboratories). Cultures were performed following previous published protocols (Jia et al., 2016). Briefly, DRGs were dissected from embryos and then digested with 0.05% trypsin (Thermo Fisher Scientific) in neurobasal medium at 37°C for 30 min. DRG neurons were dissociated with a Pasteur pipette and then the cell suspension was passed through a 70 μm cell filter (Fisher Scientific). The cells were counted and adjusted to a concentration of 3×10^7cells/ml.

DRG neurons were cultured in a microfluidic chamber (Xona Microfluidics), which permits neurons to grow their distal axons into an axonal compartment without contamination of somata and dendrites (Jia et al., 2016; Zhang et al., 2013). Sterilized chambers were placed on dishes (35 mm, Corning) coated with poly-D-lysine (Sigma-Aldrich). The DRG neurons (6×10^5cells/chamber) were cultured in chambers in DMEM with 5% FBS for 4 hours and then the medium was replaced with neurobasal medium (Invitrogen), 2mM GlutaMax, 2% B-27, and 1% antibiotic-antimycotic (Invitrogen). 5-fluorodeoxyuridine was used to purify the neurons. On 3 day in vitro (DIV), the medium was changed with non-5-fluorodeoxyuridine neurobasal medium. The growth media was replaced every other day (Jia et al., 2016; Zhang et al., 2013).

In the primary embryonic DRG neuron study, a regular glucose (RG) medium was referred to as a medium containing 25 mM glucose (optimal glucose concentration for the culture of primary embryonic DRG neurons). High glucose (HG) medium was defined as a medium containing 45 mM glucose. Both concentrations of glucose are commonly used for the embryonic DRG neurons for in vitro hyperglycemia experiments (Jia et al., 2016; Russell et al., 1999; Russell et al., 2002; Wang et al., 2014). The effects of Tβ4 (100 ng/ml) on DRG neurons under HG conditions were measured (Wang et al., 2012).

4.10. Immunocytochemistry and axonal measurement:

Immunofluorescent staining was performed as previously reported (Wang et al., 2015a). Monoclonal antibody against phosphorylated neurofilament heavy protein (pNFH, 1:500, Covance) was used. Nuclei were counterstained with DAPI (1:5000). For axonal measurement, the length of the 15 longest axons in each chamber was measured by tracing individual axons with the MCID system at DIV5 (Jia et al., 2016; Zhang et al., 2013).

4.11. Transfection of MDEs and DRG neurons with miR-146a mimics and inhibitors:

To examine the effect of miR-146a on MDEs and DRG neurons, these cells were transfected by means of Nucleofector™ kit (Lonza) with miRIDIAN microRNA Mouse mmu-miR-146a-5p-Mimic (Dharmacon, C-310423-05-0005), miRIDIAN microRNA Mimic Negative Control (Dharmacon,CN-001000-01-05), miRIDIAN microRNA Mouse mmu-miR-146a-5p- Hairpin Inhibitor (Dharmacon, IH-310423-07-0005) and miRIDIAN microRNA Hairpin Inhibitor Negative Control (Dharmacon, IN-001005-01), following the manufacturer's protocol (Jia et al., 2016; Wang et al., 2014). Briefly, miRNA mimics, inhibitors or corresponding controls at 200 pmol/well were mixed with 100 μl of nucleofector solution. MDEs or DRG neurons were added to the transfection solution and then were transferred into a cuvette. The programs V-01 for MDEs and O-03 for DRG neurons were used for electroporation, respectively (Jia et al., 2016; Wang et al., 2014).

4.12. Quantification of mature miR-146a by Real-Time RT-PCR:

Total RNAs from tissues or cells were isolated using the miRNeasy Mini kit (Qiagen). Reverse transcription and TaqMan microRNA assay were performed on ABI 7000 and ABI ViiA 7 PCR instrument (Applied Biosystems) (Wang et al., 2014). Briefly, 15 μl of reverse transcription reactions were used, including 100 ng total RNA, 5U MultiScribe Reverse Transcriptase, 0.5 mM each of dNTPs, 1x reverse transcription buffer, 4U RNase inhibitor, and nuclease-free water. The running program was as follows: 16 °C for 30 min, 42 °C for 30 min, 85 °C for 5 min. For TaqMan assay, 20 μl qRT-PCR reactions were used, including 1x TaqMan Universal PCR Master Mix No AmpErase UNG, 1x TaqMan miRNA assay, 1.33 μl of cDNA and nuclease-free water. The running program was: 95 °C for 10 min, followed by 40 cycles at 95 °C for 15 s, and 60 °C for 1 min. Relative levels of miRNAs were calculated by means of the $2^{-\Delta\Delta C}{}_T$ method with U6 snRNA TaqMan miRNA control assay (Applied Biosystem) as the endogenous control (Livak and Schmittgen, 2001). Each sample was tested in triplicate, and at least three samples obtained from independent experiments were examined. The following hydrolysis miRNA primers were used: mmu-miR-146a-5p (mature sequence: UGAGAACUGAAUUCCAUGGGUU) (Dharmacon, MIMAT0000158). Relative levels of miRNA were calculated by means of the formula $2^{-\Delta\Delta C}{}_T$ after normalizing $\Delta\Delta C_T$ values to a reference miRNA U6.

4.13. Quantification of mRNA by Real-Time RT-PCR:

The reverse transcription was performed using M-MLV reverse-transcriptase (Invitrogen). The qRT-PCR was performed using the SYBR green real-time PCR method on a ViiA7 Instrument (Applied Biosystems) (Wang et al., 2014). The mRNA of Heat shock cognate protein 70 (HSC70) was used as a reference gene. The primers are: HSC70 (FWD,

GGCACCACCTACTCCTGTGT; REV, TCTGTGTCCGTGAAAGCAAC), IRAK1 (FWD, GAGACCCTTGCTGGTAGAG; REV, GCTACACCCACCCACAGAGT), TRAF6 (FWD, GCCCAGGCTGTTCATAATG; REV, CGGATCTGATGGTCCTGT), NFkB (FWD: CAGACCTTCGGTTGGAAGAG; REV: TCCTTCACAGCATTTGCATC), MCP-1(FWD:CTGCTACTCATTCACCAGCAAG;REV:CTCTCTCTTGAGCTTGGTGACA), VCAM-1 (FWD:CAGGTGGAGGTCTACTCATTCC; REV: CTCCAGATGGTCAAAGGGATAC). Relative levels of mRNAs were calculated using the $2^{-\Delta\Delta C}{}_{T}$ method (Livak and Schmittgen, 2001). Each sample was tested in triplicate.

4.14. Western blot analysis:

Western blot was performed as in published protocols (Wang et al., 2012; Wang, 2014). Briefly, equal amounts of protein extracts were separated by 10% SDS-polyacrylamide gel. The proteins were then transferred to nitrocellulose membranes, and the following antibodies were used: rabbit anti-IRAK1 (1:1000, Santa Cruz), rabbit anti-TRAF6 (1:1000, Santa Cruz), mouse anti-phospho-NF-κB p65 (1:1000, Cell Signaling Technology), mouse anti-vascular cell adhesion molecule-1 (VCAM-1, 1:500, Santa Cruz), rabbit anti-monocyte chemotactic protein-1 (MCP-1, 1:1000, Abcam) and rabbit anti-β-actin (1:10000, Abeam). Protein levels of β-actin were used as the internal controls. The band density was analyzed using Scion Image analysis program (Scion Image). At least 3 individual experiments were performed.

4.15. Statistical analysis:

Data were evaluated for normality and illustrated as mean±SE. GEE Global Test was used to test Tβ4 effect on functional recovery measured by MCV, SCV and Planter tests at day 56 after treatment. The repeated measure analysis of variance (ANCOVA) was used to study treatment effect in individual functional tests over time. The analysis started testing for group by time interaction, followed by the testing the main effect of group and subgroup analyses.

Two-sample t-test or analysis of variance (ANOVA) was used to test the group differences in immunostaining, biochemistry and Western blot measurements, respectively. The same analytical approaches were used to test effect of diabetes, compared to the normal controls. A p-value <0.05 was taken as significant.

Acknowledgements

The authors thank Landschoot-Ward Julie, and Qing-e Lu for their technical assistance and Deborah Jewell for secretarial support.

Funding

This work was supported by the National Institutes of Health Grants: NINDS grants RO1 NS075084 (LW), NIDDK RO1 DK097519 (LW) and NIDDK RO1 RDK102861A (XSL). The funders had no role in study design, data collection and analysis, decision to publish, or preparation of the manuscript.

Abbreviations:

Tβ4	Thymosin beta 4

Db/db mice	BKS. Cg-*m*+/+*Lepr*^{db}/*J mice*
IRAK1	IL-1R–associated kinase 1
TRAF6	tumor necrosis factor (TNFR)-associated factor 6
NFkB	Nuclear factor kappa-light-chain-enhancer of activated B cells
VCAM-1	Vascular cell adhesion molecule-1
MCP-1	Monocyte chemotactic protein-1
MCV	Motor nerve conduction velocities
SCV	Sensory nerve conduction velocities
DRG	Dorsal root ganglion
LDF	Laser Doppler Flowmetry
FITC	Fluorescein isothiocyanate
OCT	Optimum cutting temperature
MCID	Micro Computer Imaging Device
PGP 9.5	Protein gene product 9.5
DAPI	4′, 6-Diamidino-2-phenylindole
IgG	Immunoglobulin G
IENF	Intraepidermal nerve fiber
ANCOVA	Analysis of covariance
GEE	Generalized estimating equations
ANOVA	Analysis of variance

References

Andersen HH, Duroux M, Gazerani P, 2014 MicroRNAs as modulators and biomarkers of inflammatory and neuropathic pain conditions. Neurobiol Dis 71, 159–68. [PubMed: 25119878]

Balasubramanyam M, Aravind S, Gokulakrishnan K, Prabu P, Sathishkumar C, Ranjani H, Mohan V, 2011 Impaired miR-146a expression links subclinical inflammation and insulin resistance in Type 2 diabetes. Mol Cell Biochem 351, 197–205. [PubMed: 21249428]

Baldeon RL, Weigelt K, de Wit H, Ozcan B, van Oudenaren A, Sempertegui F, Sijbrands E, Grosse L, Freire W, Drexhage HA, Leenen PJ, 2014 Decreased serum level of miR-146a as sign of chronic inflammation in type 2 diabetic patients. PLoS One. 9, e115209. [PubMed: 25500583]

Bhaumik D, Scott GK, Schokrpur S, Patil CK, Campisi J, Benz CC, 2008 Expression of microRNA-146 suppresses NF-kappaB activity with reduction of metastatic potential in breast cancer cells. Oncogene 27, 5643–7. [PubMed: 18504431]

Bilir B, Tulubas F, Bilir BE, Atile NS, Kara SP, Yildirim T, Gumustas SA, Topcu B, Kaymaz O, Aydin M, 2016 The association of vitamin D with inflammatory cytokines in diabetic peripheral neuropathy. J Phys Ther Sci 28, 2159–63. [PubMed: 27512288]

Cheng HS, Sivachandran N, Lau A, Boudreau E, Zhao JL, Baltimore D, Delgado-Olguin P, Cybulsky MI, Fish JE, 2013 MicroRNA-146 represses endothelial activation by inhibiting pro-inflammatory pathways. EMBO Mol Med 5, 1017–34. [PubMed: 23733368]

Chopp M, Zhang ZG, 2015 Thymosin beta4 as a restorative/regenerative therapy for neurological injury and neurodegenerative diseases. Expert Opin Biol Ther 15 Suppl 1, S9–12. [PubMed: 25613458]

Ciccacci C, Morganti R, Di Fusco D, D'Amato C, Cacciotti L, Greco C, Rufini S, Novelli G, Sangiuolo F, Marfia GA, Borgiani P, Spallone V, 2014 Common polymorphisms in MIR146a, MIR128a and MIR27a genes contribute to neuropathy susceptibility in type 2 diabetes. Acta Diabetol 51, 663–71. [PubMed: 24682535]

Davidson EP, Coppey LJ, Shevalye H, Obrosov A, Yorek MA, 2018 Vascular and Neural Complications in Type 2 Diabetic Rats: Improvement by Sacubitril/Valsartan Greater Than Valsartan Alone. Diabetes. 67, 1616–1626. [PubMed: 29941448]

Doupis J, Lyons TE, Wu S, Gnardellis C, Dinh T, Veves A, 2009 Microvascular reactivity and inflammatory cytokines in painful and painless peripheral diabetic neuropathy. J Clin Endocrinol Metab. 94, 2157–63. [PubMed: 19276232]

Evans MA, Smart N, Dube KN, Bollini S, Clark JE, Evans HG, Taams LS, Richardson R, Levesque M, Martin P, Mills K, Riegler J, Price AN, Lythgoe MF, Riley PR., 2013 Thymosin beta4-sulfoxide attenuates inflammatory cell infiltration and promotes cardiac wound healing. Nat Commun 4, 2081. [PubMed: 23820300]

Garcia AI, Buisson M, Bertrand P, Rimokh R, Rouleau E, Lopez BS, Lidereau R, Mikaelian I, Mazoyer S, 2011 Down-regulation of BRCA1 expression by miR-146a and miR-146b-5p in triple negative sporadic breast cancers. EMBO Mol Med 3, 279–90. [PubMed: 21472990]

Gong Q, Lu Z, Huang Q, Ruan L, Chen J, Liang Y, Wang H, Yue Y, Feng S, 2015 Altered microRNAs expression profiling in mice with diabetic neuropathic pain. Biochem Biophys Res Commun 456, 615–20. [PubMed: 25498543]

Guan R, Purohit S, Wang H, Bode B, Reed JC, Steed RD, Anderson SW, Steed L, Hopkins D, Xia C, She JX, 2011 Chemokine (C-C motif) ligand 2 (CCL2) in sera of patients with type 1 diabetes and diabetic complications. PLoS One. 6, e17822. [PubMed: 21532752]

Hocaoglu-Emre FS, Saribal D, Yenmis G, Guvenen G, 2017 Vascular Cell Adhesion Molecule 1, Intercellular Adhesion Molecule 1, and Cluster of Differentiation 146 Levels in Patients with Type 2 Diabetes with Complications. Endocrinol Metab (Seoul). 32, 99–105. [PubMed: 28345319]

Hou J, Wang P, Lin L, Liu X, Ma F, An H, Wang Z, Cao X, 2009 MicroRNA-146a feedback inhibits RIG-I-dependent Type I IFN production in macrophages by targeting TRAF6, IRAK1, and IRAK2. J Immunol 183, 2150–8. [PubMed: 19596990]

Ii M, Nishimura H, Kusano KF, Qin G, Yoon YS, Wecker A, Asahara T, Losordo DW, 2005 Neuronal nitric oxide synthase mediates statin-induced restoration of vasa nervorum and reversal of diabetic neuropathy. Circulation. 112, 93–102. [PubMed: 15983249]

Jia L, Wang L, Chopp M, Zhang Y, Szalad A, Zhang ZG, 2016 MicroRNA 146a locally mediates distal axonal growth of dorsal root ganglia neurons under high glucose and sildenafil conditions. Neuroscience. 329, 43–53. [PubMed: 27167084]

Kantharidis P, Wang B, Carew RM, Lan HY, 2011 Diabetes complications: the microRNA perspective. Diabetes. 60, 1832–7. [PubMed: 21709278]

Kawamura N, Dyck PJ, Schmeichel AM, Engelstad JK, Low PA, Dyck PJ, 2008 Inflammatory mediators in diabetic and non-diabetic lumbosacral radiculoplexus neuropathy. Acta Neuropathol 115, 231–9. [PubMed: 18064475]

King GL, 2008 The role of inflammatory cytokines in diabetes and its complications. J Periodontol 79, 1527–34. [PubMed: 18673007]

Landry DB, Couper LL, Bryant SR, Lindner V, 1997 Activation of the NF-kappa B and I kappa B system in smooth muscle cells after rat arterial injury. Induction of vascular cell adhesion

molecule-1 and monocyte chemoattractant protein-1. Am J Pathol 151, 1085–95. [PubMed: 9327742]

Liu XS, Fan B, Szalad A, Jia L, Wang L, Wang X, Pan W, Zhang L, Zhang R, Hu J, Zhang XM, Chopp M, Zhang ZG, 2017 MicroRNA-146a Mimics Reduce the Peripheral Neuropathy in Type II Diabetic Mice. Diabetes.

Livak KJ, Schmittgen TD, 2001 Analysis of relative gene expression data using real-time quantitative PCR and the 2(-Delta Delta C(T)) Method. Methods. 25, 402–8. [PubMed: 11846609]

Lorenzen J, Kumarswamy R, Dangwal S, Thum T, 2012 MicroRNAs in diabetes and diabetes-associated complications. RNA Biol. 9, 820–7. [PubMed: 22664916]

Lu Y, Cao DL, Jiang BC, Yang T, Gao YJ, 2015 MicroRNA-146a-5p attenuates neuropathic pain via suppressing TRAF6 signaling in the spinal cord. Brain Behav Immun 49, 119–29. [PubMed: 25957028]

Morris DC, Chopp M, Zhang L, Lu M, Zhang ZG, 2010 Thymosin beta4 improves functional neurological outcome in a rat model of embolic stroke. Neuroscience. 169, 674–82. [PubMed: 20627173]

Natarajan R, Putta S, Kato M, 2012 MicroRNAs and diabetic complications. J Cardiovasc Transl Res 5, 413–22. [PubMed: 22552970]

Navarro JF, Mora C, 2005 Role of inflammation in diabetic complications. Nephrol Dial Transplant 20, 2601–4. [PubMed: 16188894]

Newton K, Dixit VM, 2012 Signaling in innate immunity and inflammation. Cold Spring Harb Perspect Biol 4.

Norido F, Canella R, Zanoni R, Gorio A, 1984 Development of diabetic neuropathy in the C57BL/Ks (db/db) mouse and its treatment with gangliosides. Exp Neurol 83, 221–32. [PubMed: 6692864]

Pande M, Hur J, Hong Y, Backus C, Hayes JM, Oh SS, Kretzler M, Feldman EL, 2011 Transcriptional profiling of diabetic neuropathy in the BKS db/db mouse: a model of type 2 diabetes. Diabetes. 60, 1981–9. [PubMed: 21617178]

Pickup JC, 2004 Inflammation and activated innate immunity in the pathogenesis of type 2 diabetes. Diabetes Care. 27, 813–23. [PubMed: 14988310]

Rahman MH, Jha MK, Kim JH, Nam Y, Lee MG, Go Y, Harris RA, Park DH, Kook H, Lee IK, Suk K, 2016 Pyruvate Dehydrogenase Kinase-mediated Glycolytic Metabolic Shift in the Dorsal Root Ganglion Drives Painful Diabetic Neuropathy. J Biol Chem 291, 6011–25. [PubMed: 26769971]

Russell JW, Sullivan KA, Windebank AJ, Herrmann DN, Feldman EL, 1999 Neurons undergo apoptosis in animal and cell culture models of diabetes. Neurobiol Dis 6, 347–63. [PubMed: 10527803]

Russell JW, Golovoy D, Vincent AM, Mahendru P, Olzmann JA, Mentzer A, Feldman EL, 2002 High glucose-induced oxidative stress and mitochondrial dysfunction in neurons. Faseb J. 16, 1738–48. [PubMed: 12409316]

Santra M, Zhang ZG, Yang J, Santra S, Santra S, Chopp M, Morris DC, 2014 Thymosin beta4 up-regulation of microRNA-146a promotes oligodendrocyte differentiation and suppression of the Toll-like proinflammatory pathway. J Biol Chem 289, 19508–18. [PubMed: 24828499]

Sima AA, Robertson DM, 1978 Peripheral neuropathy in mutant diabetic mouse [C57BL/Ks (db/db)]. Acta Neuropathol 41, 85–9. [PubMed: 636848]

Taganov KD, Boldin MP, Chang KJ, Baltimore D, 2006 NF-kappaB-dependent induction of microRNA miR-146, an inhibitor targeted to signaling proteins of innate immune responses. Proc Natl Acad Sci U S A 103, 12481–6. [PubMed: 16885212]

Wang L, Chopp M, Szalad A, Liu Z, Lu M, Zhang L, Zhang J, Zhang RL, Morris D, Zhang ZG, 2012 Thymosin beta4 promotes the recovery of peripheral neuropathy in type II diabetic mice. Neurobiol Dis 48, 546–55. [PubMed: 22922221]

Wang L, 2014 The role of miR-146a in dorsal root ganglia neurons of experimental diabetic peripheral neuropathy. 259, 155–63.

Wang L, Chopp M, Szalad A, Zhang Y, Wang X, Zhang RL, Liu XS, Jia L, Zhang ZG, 2014 The role of miR-146a in dorsal root ganglia neurons of experimental diabetic peripheral neuropathy. Neuroscience. 259, 155–63. [PubMed: 24316060]

Wang L, Chopp M, Jia L, Lu X, Szalad A, Zhang Y, Zhang R, Zhang ZG, 2015a Therapeutic Benefit of Extended Thymosin beta4 Treatment Is Independent of Blood Glucose Level in Mice with Diabetic Peripheral Neuropathy. J Diabetes Res 2015, 173656. [PubMed: 25945352]

Wang L, Chopp M, Szalad A, Jia L, Lu X, Lu M, Zhang L, Zhang Y, Zhang R, Zhang ZG, 2015b Sildenafil ameliorates long term peripheral neuropathy in type II diabetic mice. PLoS One. 10, e0118134. [PubMed: 25689401]

Wright N.M.W.a.D.E., 2011 Inflammatory Mediators in Diabetic Neuropathy. Journal of Diabetes & Metabolism S5:004. doi:10.4172/2155-6156.S5-004

Wu QD, Wang JH, Fennessy F, Redmond HP, Bouchier-Hayes D, 1999 Taurine prevents high-glucose-induced human vascular endothelial cell apoptosis. Am J Physiol 277, C1229–38. [PubMed: 10600775]

Xiong Y, Mahmood A, Meng Y, Zhang Y, Zhang ZG, Morris DC, Chopp M, 2011 Treatment of traumatic brain injury with thymosin beta in rats. J Neurosurg 114, 102–15. [PubMed: 20486893]

Xiong Y, Zhang Y, Mahmood A, Meng Y, Zhang ZG, Morris DC, Chopp M, 2012 Neuroprotective and neurorestorative effects of thymosin beta4 treatment initiated 6 hours after traumatic brain injury in rats. J Neurosurg 116, 1081–92. [PubMed: 22324420]

Yorek MA, 2015 Vascular Impairment of Epineurial Arterioles of the Sciatic Nerve: Implications for Diabetic Peripheral Neuropathy. Rev Diabet Stud 12, 13–28. [PubMed: 26676659]

Yousefzadeh N, Alipour MR, Soufi FG, 2015 Deregulation of NF-small ka, CyrillicB-miR-146a negative feedback loop may be involved in the pathogenesis of diabetic neuropathy. J Physiol Biochem 71, 51–8. [PubMed: 25567745]

Zhang Y, Ueno Y, Liu XS, Buller B, Wang X, Chopp M, Zhang ZG, 2013 The MicroRNA-17–92 cluster enhances axonal outgrowth in embryonic cortical neurons. J Neurosci 33, 6885–94. [PubMed: 23595747]

Zhou J, Zhou S, 2014 Inflammation: therapeutic targets for diabetic neuropathy. Mol Neurobiol 49, 536–46. [PubMed: 23990376]

Zhou T, Huang YX, Song JW, Ma QM, 2015 Thymosin beta4 inhibits microglia activation through microRNA 146a in neonatal rats following hypoxia injury. Neuroreport 26, 1032–8. [PubMed: 26457369]

Highlights

- miR-146a mediates Tβ4-promoted endothelial cell function under hyperglycemia.
- miR-146a regulates Tβ4-induced axonal outgrowth under hyperglycemia.
- miR-146a contributes the therapeutic effect of Tβ4 on diabetic neuropathy.

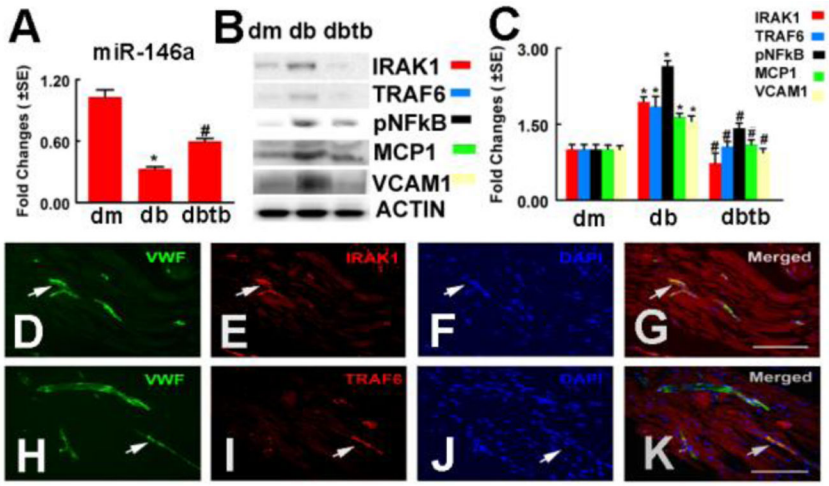

Fig.1: Tβ4 treatment increased miR-146a level and decreased IRAK1, TRAF6 and p-NFkB expression, as well as MCP-1 and VCAM-1 levels in sciatic nerve tissues.

Panels A to C show real-time RT-PCR analysis of miR-146a expression (A) and Western blot analysis of IRAK1, TRAF6 and p-NFkB, as well as MCP-1 and VCAM-1 levels in the sciatic nerve tissues, β-actin was used as an internal control (B and C). Double immunofluorescent staining shows that IRAK1 (E, G red, arrows) and TRAF6 (I, K, red, arrows) immunoreactivity were localized to vWF positive vessels (D, G, H, K green, arrows). Panels F and J show DAPI nuclear staining (blue). *$p<0.05$ and #$p<0.05$ versus the db/m mouse and the saline treated db/db mouse, respectively. n=6/group. Bar=100 μm. dm=db/m mouse; db=db/db mouse. dbtb=diabetic mouse treated with Tβ4.

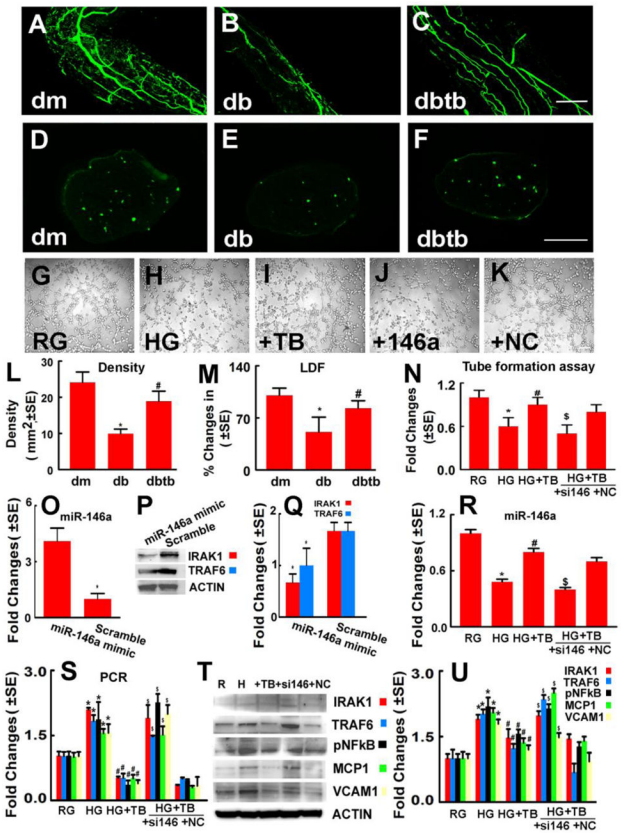

Fig.2: miR-146a mediates Tβ4-improved vascular function in the diabetic sciatic nerve.

Panels A to F show that whole-mounted (A to C) and cross sections (D to F) of the sciatic nerve tissues revealed FITC-dextran perfused vessels from a representative dm mouse (A, D), db mouse treated with saline (B, E), and db mouse treated with Tβ4 (C,F). Panels L and M show quantitative data of the density of FITC-dextran perfused vessels in cross section (L, n=6/group) and percentage changes of sciatic nerve tissue blood flow with a reference of dm mice at 100% (M, n=6/group). *p<0.05 and #p<0.05 versus the db/m mouse and the saline treated db/db mouse, respectively. Bar=100μm. dm=db/m mouse; db=db/db mouse. dbtb=diabetic mouse treated with Tβ4. Panels G to K show representative microscopic images (G-K) and quantitative data (N) of capillary-like tube formation in MDEs cultured in normal glucose (RG), high glucose (HG), high glucose with Tβ4 (HG+TB), high glucose with Tβ4 in the presence of miR-146a inhibitor (+si146) and scramble negative control (+NC). Bar in K=50μm. Panel O shows quantitative data of real-time RT-PCR analysis of miR-146a expression in MDEs. Panels P and Q show Western blot analysis of IRAK1 and TRAF6 levels in MDEs transfected with miR-146a mimics and scramble control, respectively. Panel R shows quantitative data of real-time RT-PCR analysis of miR-146a expression in MDEs. Panels S to U show quantitative data of real-time RT-PCR (S) and Western blot analysis (T and U) of IRAK1,TRAF6, p-NFkB, MCP-1 and VCAM-1 levels in MBEs under different conditions, and HSC70 and β-actin were used as internal controls, respectively. *p<0.05, #p<0.05 and $p<0.05 versus the normal glucose (RG), high glucose (HG) and scramble negative control (NC) groups, respectively. n=6/group.

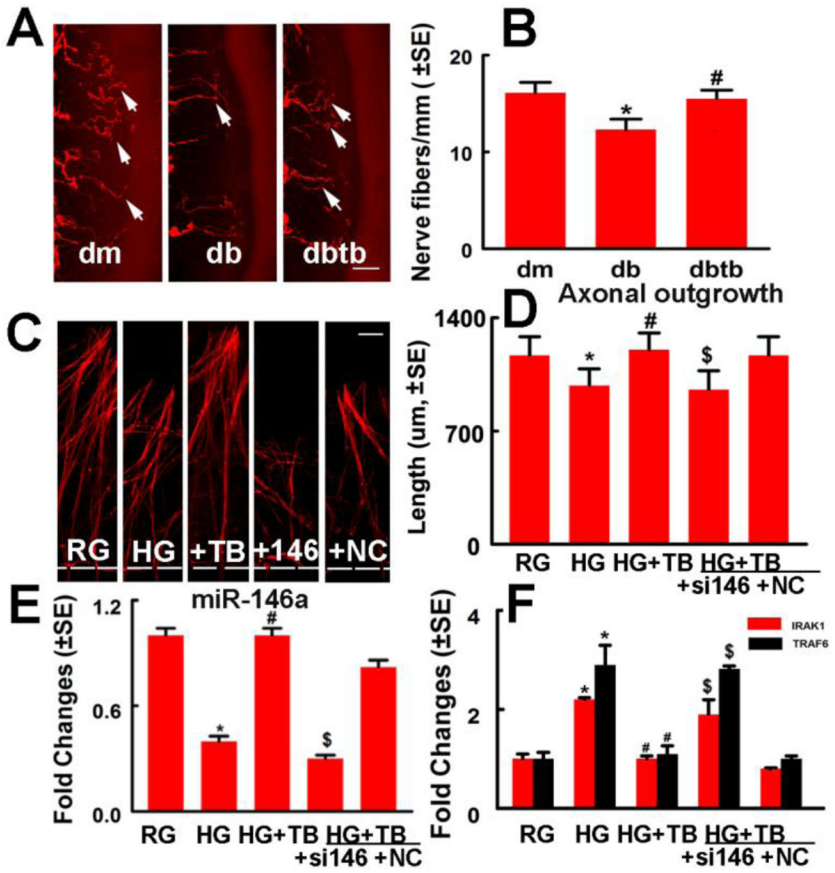

Fig.3: miR-146a mediates Tβ4-induced axonal remodeling in vivo and in vitro.

Panels A and B show PGP 9.5 immunoreactive intraepidermal nerve fibers (red, arrows) in the plantar skin from a representative non-diabetic mouse treated with saline (dm), diabetic mouse treated with saline (db) and diabetic mouse treated with Tβ4 (dbtb). Panel B shows quantitative data of intraepidermal nerve fiber density (IENFD). *p<0.05 and #p<0.05 versus the non-diabetic mouse (dm) and the diabetic mouse treated with saline (db), respectively. n=10/group. Bar=50μm. Panels C and D show representative microscopic images (C) and quantitative data (D) of axonal outgrowth in DRG neurons cultured in normal glucose (RG), high glucose (HG), high glucose with Tβ4 (+TB), high glucose with Tβ4 in the presence of miR-146a inhibitor (+si146) and scramble negative control (+NC). Panel E shows quantitative data of real-time RT-PCR analysis of miR-146a (E) and IRAK1 and TRAF6 (F) levels in DRG neurons under different conditions, and HSC70 was used as an internal reference gene (F). *p<0.05, #p<0.05 and $p<0.05 versus the normal glucose (RG), high glucose (HG) and scramble negative control (NC) groups, respectively. n=6/group. Bar in C =100μm

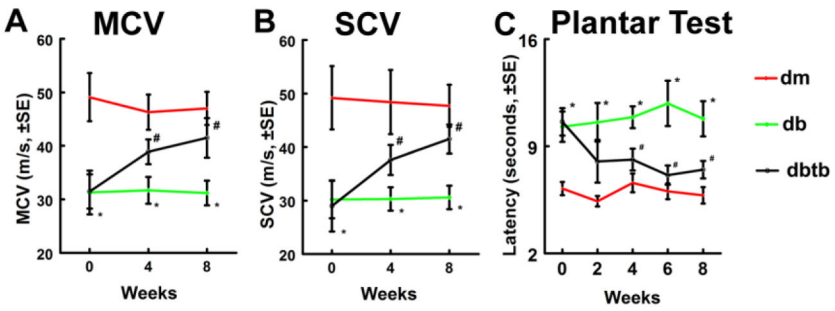

Fig.4: Effect of Tβ4 on neurological function in diabetic db/db mice.

Treatment of db/db mice with Tβ4 improved neurological function measured by MCV (A), SCV (B) and Plantar Test (C). *$p<0.05$ and #$p<0.05$ versus the db/m mouse and the db/db mouse treated with saline, respectively. n=10/group. dm=db/m mouse; db=db/db mouse. dbtb=diabetic mouse treated with Tβ4.

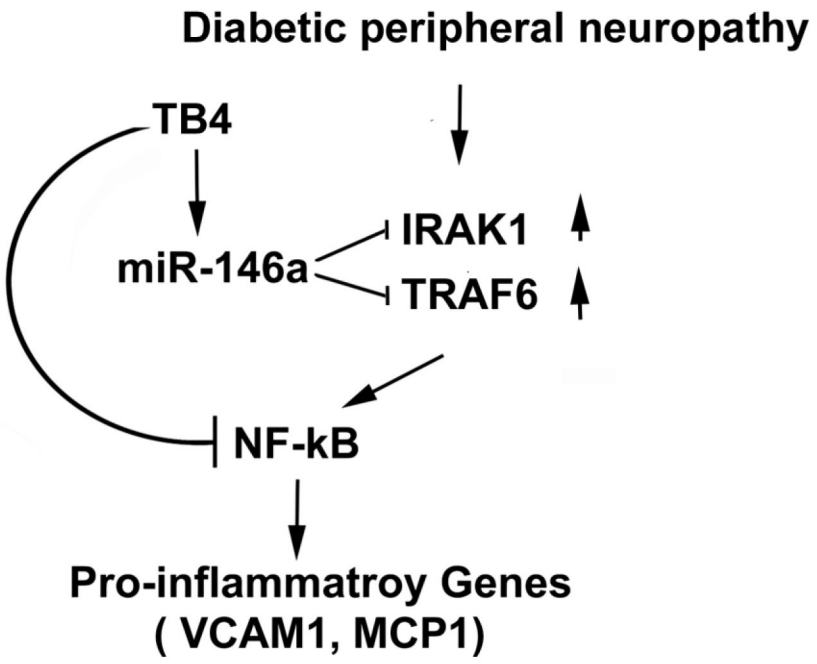

Fig.5:

A schematic shows potential interaction of miR-146a increased by Tβ4 with its target genes and downstream pro-inflammatory proteins. Diabetic peripheral neuropathy down-regulates miR-146a, upregulates IRAK1 and TRAF6, and activates downstream NFkB. Tβ4-elevated miR-146a represses IRAK1 and TRAF6, which results in attenuation of NFkB activation and pro-inflammatory genes VCAM-1 and MCP-1.

Table 1.

Effect of Tβ4 on body weight

	Weight, g		
Groups	**0 w**	**4 w**	**8 w**
dm-saline	29.6±0.7 *	29.9±0.8 *	28.4±0.7 *
db-saline	57.1±1.8	54.4±3.15	54.2±1.8
db-Tβ4	57.3±1.5	51.7±2.3	53.1±2.0

Values are mean±SE.

* p<0.01 versus db+saline group. n=10/group. w indicates the week before and after the treatment, respectively.

Table 2.

Effect of Tβ4 on blood glucose

	Blood glucose (g/dl)		
Groups	**0 w**	**4 w**	**8 w**
dm-saline	139±7.2 *	141±4.3 *	126±5.4 *
db-saline	481±19.4	522±19.5	475±19.9
db-Tβ4	523±12.7	514±16.1	522±26.0

Values are mean±SE.

* p<0.01 versus db+saline group. n=10/group. w indicate that the week before and after the treatment, respectively.